

# Development of high-power electrodes for a liquid-feed direct methanol fuel cell

C. Lim, C.Y. Wang\*

*Departments of Mechanical Engineering and Materials Science & Engineering, Electrochemical Engine Center (ECEC),  
The Pennsylvania State University, 338 Reber Building, University Park, PA 16802, USA*

Received 5 July 2002; accepted 23 September 2002

## Abstract

Based upon Nafion 112 membrane, membrane-electrode assemblies for a liquid-feed direct methanol fuel cell (DMFC) were fabricated by using a novel method of modified Nafion solution and tape-casting, with unsupported Pt-Ru as an anode catalyst and carbon supported 40 wt.% Pt as a cathode catalyst. The amounts of catalyst loading were controlled to be 4 mg/cm<sup>2</sup> in the anode and 1.3 mg/cm<sup>2</sup> in the cathode. Morphological characteristics of anode and cathode were examined by scanning electron microscopy (SEM). A time-delayed activation effect was found in single cell tests and attributed to time-dependent wetting behavior of Nafion polymers within both catalyst layers. A high compression of the single cell leads to a remarkable decrease in diffusion-limiting current density, caused by hydrophilic broken fibers and cleavage-like defects generated during excessive compression of the cell. A maximum power density of 0.21 W/cm<sup>2</sup> is achieved in 2 M CH<sub>3</sub>OH solution at 90 °C under the operating condition of non-pressurized anode side and non-humidified air pressurized to 15 psi.

© 2002 Elsevier Science B.V. All rights reserved.

*Keywords:* Direct methanol fuel cells; Membrane-electrode assembly (MEA); Polymer electrolytes; High power

## 1. Introduction

Despite significant recent efforts to improve the power performance of pure hydrogen or reformate gas proton exchange membrane fuel cells (PEMFCs), there are still many technological hurdles to overcome before the commercialization as stationary and vehicle power sources, due largely to difficulties in hydrogen supply infrastructure or fuel reforming technology with clean-up of impurities such as carbon monoxide and sulfur compounds. In the meanwhile, the PEM-based direct methanol fuel cell (DMFC) is receiving increasingly more attraction due to its much simpler peripheral units than those of the PEMFC system, such as easy fuel delivery and storage, no need for reforming, humidification and stack cooling, and favorable transient power capability.

Depending on fuel operating strategy, the DMFC technology can be categorized into two groups. One is a vapor-feed DMFC operating above a cell temperature of 100 °C at the atmospheric pressure and the other is a liquid-feed DMFC operating below 100 °C. As mentioned by Baldauf and Pridel [1], it is not practically promising to operate the DMFC at temperatures higher than 110 °C, highly pressurized air above

1.5 bar, needless to say, to operate with pressurized oxygen. The methanol crossover rate is reported to be dependent strongly on the thickness of the polymer membrane [2,3]. The thicker the membrane is, the less the methanol crossover becomes. However, the thick membrane reduces the power density due to its high ohmic loss, trading off with the low methanol crossover. The maximum power density obtained with Nafion 117 is reported to be slightly less than 0.1 W/cm<sup>2</sup> in practical operating conditions [1]. Recently, the fuel utilization up to 90% is reported even with Nafion 112 [4,5] by achieving a high-power density in 1 M methanol solution, i.e. reacting the methanol efficiently in the anode catalyst layer before it crosses over the membrane.

The objective of this study is to fabricate a membrane-electrode assembly (MEA) tailored for DMFC with a novel method of catalyst wet-processing and to attain a high-power density with Nafion 112 membrane in the practically promising operating conditions, i.e. below 100 °C, near ambient pressure and non-humidified air.

## 2. Experimental

Both the anode and cathode consist of a backing layer, a microporous layer and a catalyst layer. A commercial

\* Corresponding author. Tel.: +1-814-863-4762; fax: +1-814-863-4848.  
E-mail address: cxw31@psu.edu (C.Y. Wang).

20 wt.% FEP wet-proofed carbon papers (Toray 090, E-Tek) of 0.26 mm in thickness were employed as the backing layers for both anode and cathode. To prepare the microporous layer smoothing out the substrate surface, Vulcan XC72R (Cabot) carbon black was dispersed into a water/alcohol mixture containing 40 wt.% of Teflon (TFE 30, Dupont) based on weight gain after drying. The resultant slurry was spread on the carbon paper by using a gap-adjustable knife-blade, followed by drying at 100 °C and sintering at 360 °C for 15 min. The amount of loading of carbon and Teflon in the microporous layer was about 2 mg/cm<sup>2</sup>.

Next, a commercial 5 wt.% Nafion solution (EW1100, Aldrich) was treated with diluted sodium hydroxide solution, resulting in Na<sup>+</sup> form of Nafion solution. This is followed by mixing and then heating with a viscous organic solvent, resulting in a solvent-substituted Nafion solution. A slurry for the catalyst layer was prepared by dispersing unsupported Pt-Ru black (HiSPEC 6000, Pt:Ru = 1:1 atomic ratio, Alfa Aesar) for an anode or carbon supported Pt (40 wt.% Pt on Vulcan XC72R, E-Tek) for a cathode into the solvent-substituted Nafion solution. The resultant slurry was spread on the microporous layer-coated carbon paper also by using the knife-blade, cured in an inert atmospheric oven, re-protonated to H<sup>+</sup> form of Nafion in diluted sulfuric acid and then dried again in the oven. This leaves Pt-Ru loading of 4 mg/cm<sup>2</sup> and Nafion loading of 1 mg/cm<sup>2</sup> in the anode catalyst layer, and Pt loading of 1.3 mg/cm<sup>2</sup> and Nafion loading of 1 mg/cm<sup>2</sup> in the cathode catalyst layer.

A commercial Nafion 112 membrane (EW 1100, Dupont) was treated according to the membrane cleaning procedure [6]. After trimming the catalyzed electrodes for the anode and cathode, respectively, these were positioned on both sides of the pre-cleaned Nafion 112 and hot pressed to form a unit of MEA at 125 °C and 100 kg/cm<sup>2</sup> for 3 min. The MEA was immersed into water at least overnight before installing it into a single cell fixture (consisting of graphite plates with an active area of 5 cm<sup>2</sup>, Electrochem. Inc.) having three-pass serpentine flow channels with both width and depth of 0.7 mm. A diluted methanol solution was fed into the anode inlet at a flow rate of 3 cm<sup>3</sup>/min by a peristaltic pump without pre-heating and back pressurization. Non-humidified room temperature air was fed into a cathode inlet at a flow rate of 600 sccm and pressurized at 15 psi by a back pressure regulator.

Polarization curves were obtained by using an Arbin BT + 4 Testing System in a galvanodynamic polarization mode at a scan rate of 3 mA/s. Anode polarization curves were measured with respect to a hydrogen-fed cathode acting as a counter electrode and simultaneously a dynamic hydrogen electrode (DHE), while cell ohmic resistances were obtained at a frequency of 1500 Hz by using a Solartron 1287 electrochemical interface in conjunction with a Solartron 1260 frequency response analyzer.

### 3. Results and discussion

Cross-sectional scanning electron microscopy (SEM) micrographs of the catalyzed anode and cathode are shown in Fig. 1a and b, respectively. Fig. 1a displays a planar microporous layer with an average thickness of 30 μm over a carbon paper substrate consisting of non-woven graphite fibers with an average diameter of 5 μm. On top of the microporous layer, an anode catalyst layer of about 20 μm in thickness consisting of unsupported Pt-Ru black and Nafion polymer is observed to be more porous than the microporous layer. A cathode catalyst layer was coated on the same microporous layer-coated carbon paper as was used in the anode. In Fig. 1b, uniform cracks and distortions, which were introduced into the dual layer of catalyst and microporous layer due to volume shrinkage of catalyst slurry during a curing step of it, were observed. The microporous layer appears to penetrate into the backing layer somewhat. A cathode catalyst layer with an average thickness of 30 μm can be seen on top of the cathode microporous layer.

To obtain reliable polarization behaviors of MEA, the activation condition of MEA needs to be specified. A time-dependent activation behavior of the MEA is presented in Fig. 2. The first polarization curve was measured at 30 min after installing and operating the single cell in 2 M methanol solution at 90 °C. After that, the MEA was kept in contact with the methanol solution for overnight and then a polarization curve was measured again at the same cell operating condition. Cell voltage increased by 75 mV at 400 mA/cm<sup>2</sup>, while the anode potential including the cell ohmic voltage drop, which is measured with respect to a hydrogen-fed cathode, decreased only by 45 mV at the same current density, indicating that both the anode and cathode catalyst layers undergo the activation process.

Nafion polymer particles within the catalyst layer act as the ionic phase only when those are moisturized enough to have high ionic conductivity. Only the catalyst particles contacting with the effective ion-conducting polymers can contribute to the electrochemical reaction as active catalytic sites. Therefore, the activation effect may be considered to come from a time-dependent wetting behavior of the Nafion polymers within the catalyst layer. Especially, it would take longer for the MEA to be fully activated in a non-humidified than in a fully-humidified oxidant fuel, because in the former case the Nafion in the cathode catalyst layer is moisturized only by the water crossing over the membrane.

Ren et al. [7] studied polarization behaviors of anode in operating DMFC by using two different types of reference electrode, i.e. a DHE subject to a galvanostatic current density of 6 mA/cm<sup>2</sup>, and a hydrogen evolution counter electrode. They found that the hydrogen evolution counter electrode has a potential higher than the DHE reference electrode in the low current density regime but lower than the DHE in the high current density regime due to noticeable polarization of the hydrogen evolution counter electrode. In the present study, the measurement of anode polarization

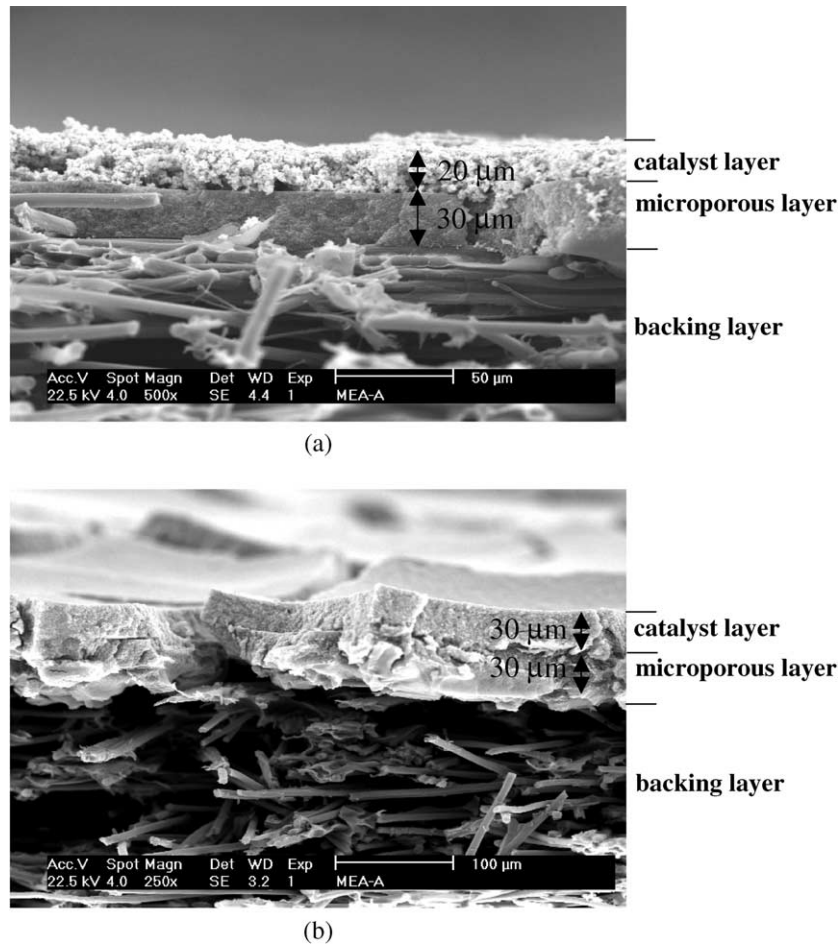


Fig. 1. Cross-sectional SEM micrographs of: (a) anode; (b) cathode. Unsupported Pt-Ru was used as the anode catalyst and carbon supported 40 wt.% Pt as the cathode catalyst.

behavior using the hydrogen evolution counter electrode was employed to diagnose polarization behaviors of the unit cell without modifications of the operating cell fixture and MEA. It should, however, be kept in mind that using the hydrogen

evolution counter electrode as a reference electrode does not give precise information to separate the cell voltage into anodic and cathodic overpotential contributions.

In an attempt to study the effect of cell compression, MEAs were subjected to two different degrees of compression by using incompressible Teflon gaskets having different thicknesses, i.e. 100 and 200 μm. Considering the final thickness of the catalyzed electrode is about 300 μm, both the anode and cathode would experience a thickness reduction of about 2/3 and 1/3 in cases of a highly-compressed MEA and mildly-compressed MEA, respectively. The effect of cell compression on power performance of MEA is shown in Fig. 3. The highly-compressed MEA showed a kinetic and diffusion-limiting current much lower than that of the mildly-compressed one, while the anode polarization curves measured in reference to the hydrogen evolving cathode showed the similar behavior, indicating that the decrease of cell performance in the highly-compressed MEA is mainly attributed from a degrading cathode.

After disassembling the highly-compressed cell, a surface and a cross-sectional micrographs representing morphologies of the gas diffusion backing layer contacted with a

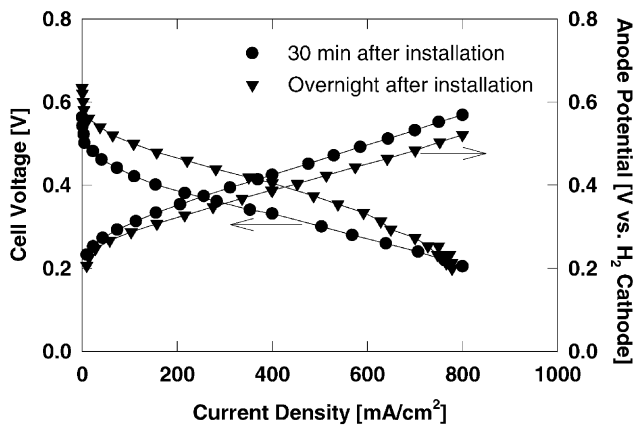


Fig. 2. Effect of time elapsed after installing MEA into single cell on the cell and anode polarization characteristics measured in 2 M CH<sub>3</sub>OH at 90 °C under the conditions of 0 psi anode side and 15 psi non-humidified air.

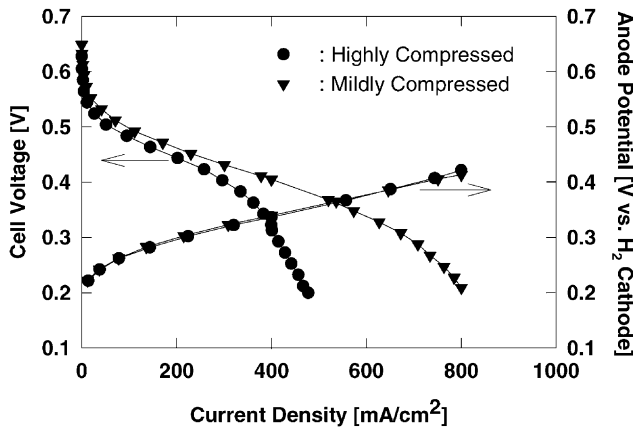
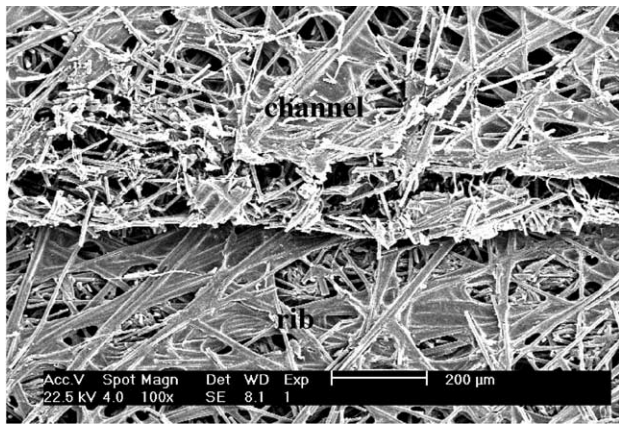
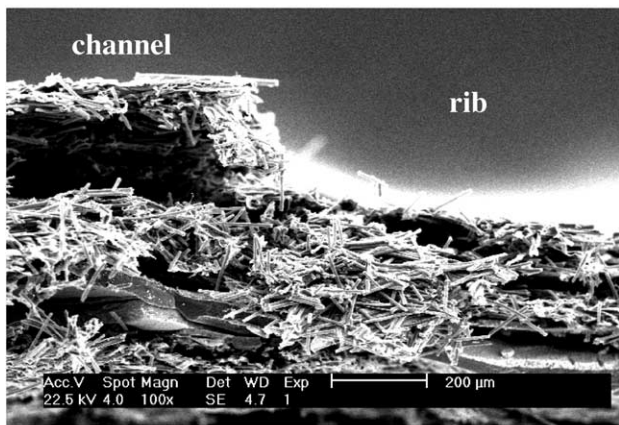


Fig. 3. Effect of cell compression on the cell and anode polarization characteristics measured in 2 M CH<sub>3</sub>OH at 90 °C under the conditions of 0 psi anode side and 15 psi non-humidified air.

channel and a rib on a flow plate were taken by SEM as presented in Fig. 4a and b. In the middle of the micrograph shown in Fig. 4a, it is observed that graphite fibers were broken through the edge of a step between the part of



(a)

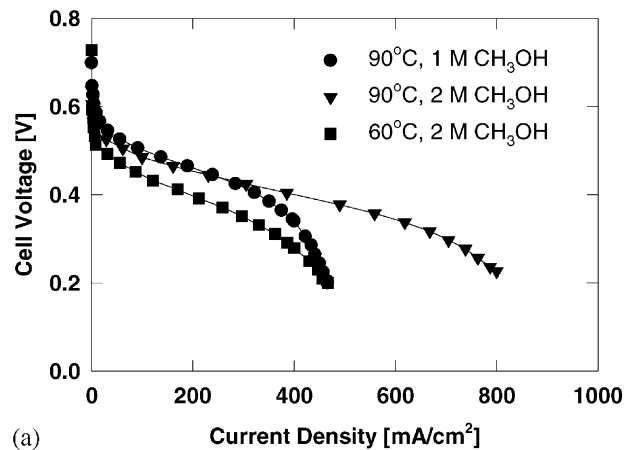


(b)

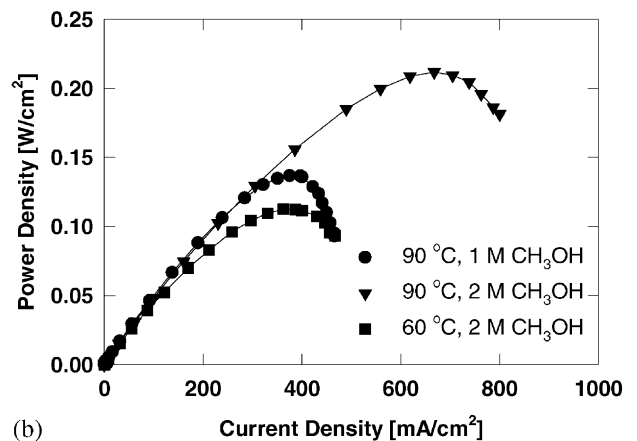
Fig. 4. SEM micrographs of: (a) surface; (b) cross-section of highly-compressed gas diffusion electrode contacted with a channel and a rib on the flow plate.

backing layer (the bottom portion of the image) compressed by the rib and the part of backing layer (the upper portion of the image) facing the channel. It is expected that these broken fibers act as hydrophilic defects and hence decrease water removal of the cathode. In Fig. 4b, the part of the backing layer compressed by the rib is seen on the right side and the part facing the channel is on the left side of the micrograph.

As can be clearly seen in Figs. 1b and 4a, the carbon paper electrode is composed of thin and long graphite fibers randomly stretching out in the in-plane direction, making the electrode tougher in the in-plane direction than in the through-plane direction. As the part of electrode is severely compressed by the rib, the part of electrode exposed to the free space of the channel is subject to a tensile force in the through-plane direction by a cantilever mechanism, leading to delamination of the backing layer as shown in the upper left region of the micrograph (Fig. 4b). These cleavage-like defects in the gas diffusion electrode are expected to significantly lower the water removal rate of the cathode as can be inferred from Fig. 3.



(a)



(b)

Fig. 5. Curves of: (a) cell voltage; (b) power density vs. current density as function of molarity of methanol and cell temperature obtained under the conditions of 0 psi, 3 cm<sup>3</sup>/min of methanol solution and 15 psi, 600 sccm of non-humidified air.



The effects of methanol concentration and cell temperature on polarization curve and power density of MEA are shown in Fig. 5a and b, respectively. In Fig. 5a, the cell voltage increased in the kinetic control regime with decreasing molarity of methanol solution, indicating that the cathode potential becomes higher due to less methanol crossover in more dilute methanol solution [7–9]. An anode potential measurement with respect to the hydrogen-fed cathode further indicated that the lower kinetic and diffusion-limiting current densities at 60 °C resulted mainly from the increased overpotential and decreased methanol transport in the anode. In Fig. 5b, a maximum power density of 0.21 W/cm<sup>2</sup> is achieved at 0.32 V in non-humidified and 15 psi pressurized air.

Power performance is strongly dependent on cell operating parameters and morphological characteristics of MEA. Several papers [4,5,10,11] in the literature used MEA based on Nafion 112. Arico et al. [5] studied polarization behaviors of MEA based upon home-made unsupported Pt-Ru as an anode catalyst and carbon supported 30 wt.% Pt/C as a cathode catalyst, with a catalyst loading of 2 mg/cm<sup>2</sup> in each. They could achieve 0.24 W/cm<sup>2</sup> in 2 M methanol solution at 0.3 V and 130 °C, but the power density becomes to 0.12 W/cm<sup>2</sup> even in 30 psi pressurized air when the cell temperature is lowered to 90 °C. To date, the highest performance below 100 °C was reported to be 0.2 W/cm<sup>2</sup> at 0.3 V by Ren et al. [4] where the cell temperature is 80 °C with 1 M methanol and a 30 psi air electrode.

To make anode polarization curves independent of catalyst loading, operating conditions in the cathode, and the type of membrane, anode polarization curves normalized by the mass of anode catalyst are shown in Fig. 6 after correcting cell ohmic drop on the anode polarization curves as measured with respect to the hydrogen-fed cathode. The cell ohmic resistances at 60 and 90 °C in 2 M methanol

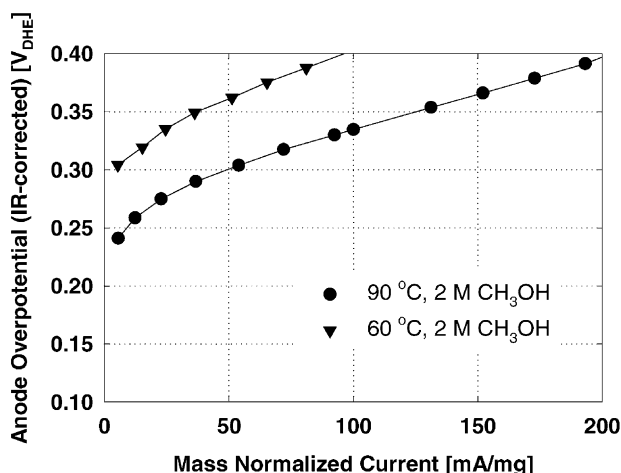


Fig. 6. IR-corrected anode overpotential vs. mass-normalized current obtained with 4 mg/cm<sup>2</sup> of unsupported Pt-Ru loaded anode under the conditions of 0 psi, 3 cm<sup>3</sup>/min of methanol solution and 15 psi, 600 sccm of non-humidified air.

solution were estimated to be 0.12 and 0.09 Ω cm<sup>2</sup>, respectively. The resulting anode mass activity consisting of 4 mg/cm<sup>2</sup> of unsupported Pt-Ru is 125 mA/mg in 2 M methanol solution at 0.35 V in the present study. This value is compared to 70 mA/mg [12] which was obtained in 1.5 M methanol solution at 0.35 V with respect to relative hydrogen electrode (RHE) and 90 °C based on 6 mg/cm<sup>2</sup> unsupported Pt-Ru loaded anode.

The type of catalyst has important effect on power performance of MEA in DMFC [12,13]. It was known that the anode with carbon-supported catalyst reaches a plateau in power performance at around 0.5–0.7 mg/cm<sup>2</sup> and further increasing catalyst loading does not have positive effect on the power performance. On the other hand, the power performance of anode with unsupported catalyst increases with the catalyst loading at least up to 6 mg/cm<sup>2</sup>. Therefore, it appears possible to use the unsupported catalyst in the anode to attain a high-power performance in DMFC at the expense of high catalyst loading.

According to theoretical calculations [13], an unsupported Pt-Ru catalyst loading of 4 mg/cm<sup>2</sup> results in a 5 μm thick catalyst layer assuming the layer porosity of 0.5. However, the thickness of the anode catalyst layer shown in Fig. 1a is estimated to be 20 μm, indicating that the porosity of the anode catalyst layer fabricated in this study is probably much higher than 0.5. The high porosity should be helpful for methanol or water to reach and for carbon dioxide to leave the catalyst layer. Also, it is noteworthy that the anode catalyst layer is quite planar owing to the planar microporous under layer, possibly contributing to a uniform current distribution in the anode.

#### 4. Conclusions

The membrane-electrode assembly, consisting of unsupported Pt-Ru as the anode catalyst, carbon supported 40 wt.% Pt/C as the cathode catalyst and Nafion 112 membrane, was fabricated by using the novel method of tape-casting in conjunction with a modified Nafion solution and showed the power density of 0.21 W/cm<sup>2</sup> in 2 M CH<sub>3</sub>OH at 90 °C under the condition of non-preheated and non-pressurized methanol solution, and non-humidified air back-pressurized to 15 psi. The anode catalyst layer in this study was characterized to be morphologically planar and porous.

#### Acknowledgements

The authors would like to thanks Prof. Matthew M. Mench and Dr. Venkat Srinivasan of ECEC for the helpful discussions and facilities set-up. Financial support from US Department of Transportation, Pennsylvania Department of Environmental Protection, and National Science Foundation is gratefully acknowledged.

**References**

- [1] M. Baldauf, W. Pridel, J. Power Sources 84 (1999) 161.
- [2] S.R. Narayanan, A. Kindler, B. Jeffries-Nakamura, W. Chun, H. Frank, M. Smart, T.I. Valdez, S. Surampudi, G. Halpert, Annu. Battery Conf. Appl. Adv. 11 (1996) 113.
- [3] D.H. Jung, C.H. Lee, C.S. Kim, D.R. Shin, J. Power Sources 71 (1998) 169.
- [4] X. Ren, P. Zelenay, S. Thomas, J. Davey, S. Gottesfeld, J. Power Sources 86 (2000) 111.
- [5] A.S. Arico, P. Creti, E. Modica, G. Monforte, V. Baglio, V. Antonucci, Electrochim. Acta 45 (2000) 4319.
- [6] D. Weng, J.S. Wainright, U. Landau, R.F. Savinell, J. Electrochem. Soc. 143 (1996) 1260.
- [7] X. Ren, T.E. Springer, S. Gottesfeld, J. Electrochem. Soc. 147 (2000) 92.
- [8] M.K. Ravikumar, A.K. Shukla, J. Electrochem. Soc. 143 (1996) 2601.
- [9] A. Heinzl, V.M. Barragan, J. Power Sources 84 (1999) 70.
- [10] X. Ren, M.S. Wilson, S. Gottesfeld, J. Electrochem. Soc. 143 (1996) L12.
- [11] A.S. Arico, A.K. Shukla, K.M. El-khatib, P. Creti, V. Antonucci, J. Appl. Electrochem. 29 (1999) 671.
- [12] L. Liu, C. Pu, R. Viswanathan, Q. Fan, R. Liu, E.S. Smotkin, Electrochim. Acta 43 (1998) 3657.
- [13] J.T. Wang, R.F. Savinell, in: Proceedings of the Symposium on Electrode Materials and Processes for Energy Conversion and Storage, vol. 94-23, The Electrochemistry Society Inc., 1994, p. 326.